JCIM JOURNAL OF CHEMICAL INFORMATION AND MODELING

pubs.acs.org/jcim Article

Molecular View on the Impact of DHA Molecules on the Physical Properties of a Model Cell Membrane

Xiu Li, Shiying Zhou, and Xubo Lin*

Cite This: https://doi.org/10.1021/acs.jcim.2c00074 Read Online

ACCESS | Metrics & More | Article Recommendations | Supporting Information

ABSTRACT: Docosahexaenoic acid (DHA) is a ω-3 polyunsaturated fatty acid, which can be uptaken by cells and is essential for proper neuronal and retinal function. However, the detailed physical impact of DHA molecules on the plasma membrane is still unclear. Hence, in this work, we carried out μs-scale coarse-grained molecular dynamics (MD) simulations to reveal the interactions between DHA molecules and a model cell membrane. As is known, the cell membrane can segregate into liquid-ordered (L_o) and liquid-disordered (L_d) membrane domains due to the differential interactions between lipids and proteins. In order to capture this feature, we adopted the three-component phase-separated lipid membranes and considered both anionic and neutral DHA molecules in the current work. Our results showed that DHA molecules can spontaneously self-assemble into nanoclusters, fuse with lipid membranes, and localize preferably in L_d membrane domains. During the membrane fusion process, DHA molecules can change the intrinsic transmembrane potential of the lipid membrane, and the effects of anionic DHA molecules are much more significant. Besides, the presence of DHA molecules mainly in the L_d membrane domains could regulate the differences in the lipid chain order, membrane thickness, cholesterol preference, and cholesterol flip-flop basically in a concentration-dependent manner, which further promote the stability of the intraleaflet dynamics and inhibit the interleaflet dynamics (or promote membrane domain registration) of the membrane domains. In short, the impact of DHA molecules on the physical properties of a model cell membrane on the molecular level revealed in our work will provide useful insights for understanding the biological functions of DHA molecules.

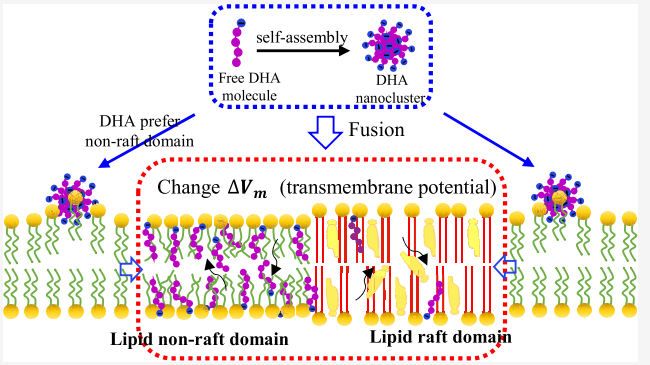

INTRODUCTION

As one kind of omega-3 polyunsaturated fatty acids (ω-3 PUFAs), docosahexaenoic acid (DHA, C22:6) plays key roles in nervous, immune, and cardiovascular systems.[1−4] It has been widely accepted that dietary DHA is essential for the development of brain and retinal functions.[5,6] Aging and dementia are usually accompanied by DHA deficiency.[7] With the rapid development of experimental techniques, the detailed molecular mechanisms for the roles of DHA molecules are gradually revealed.[8] Generally, DHA molecules are taken up by cells, then participate in a series of lipid metabolisms as well as membrane remodeling, and thus regulate cell functions.[9,10] It has been reported that DHA can incorporate into cell membrane lipids,[10,11] which may greatly increase the differences in the unsaturation and dynamics between saturated and unsaturated lipids. This further leads to the promoted formation of lipid rafts and the subsequent enhanced cellular signaling.[10,12] DHA can also directly regulate the structures and functions of proteins. For example, it can activate large-conductance Ca^{2+}-dependent K^+ channels in vascular smooth muscle cells for lowering the blood pressure,[13] or perturb certain signaling transductions to achieve the inhibition of the proliferation and growth of cancer cells.[14] However, before affecting lipid metabolism, how the free DHA molecules interact with cell membrane lipids and regulate the general physical properties of cell membrane is still far from clear.

The cell membrane consists of thousands of lipids and proteins,[15,16] which participate in a series of biological processes and play key roles in maintaining proper functions of cells. On one hand, due to the differential interactions between different lipids and proteins, the cell membrane can segregate into many membrane domains. Among them, functional ordered membrane domains are defined as "lipid rafts",[17−19] which were supposed to be nanoscale.[20−22] The stability of the lipid raft contains both the intraleaflet[23] and the interleaflet[24] dynamics, which are essential for maintaining the proper dynamics of membrane proteins.[25−28] On the other hand, the semipermeability of the cell membrane will inevitably

Received: January 20, 2022

https://doi.org/10.1021/acs.jcim.2c00074
J. Chem. Inf. Model. XXXX, XXX, XXX−XXX

cause the asymmetric distribution of either lipids or ions among intracellular and extracellular regions, which induces the transmembrane potential.[29] The membrane potential was found to be important in regulating the dynamics of membrane lipids and proteins (e.g., K-Ras[30]), and then in cell growth and proliferation.[31−34] In other words, any disruptions to the lipid raft stability and the membrane potential may induce significant changes to the dynamics of proteins and lipids, which in turn affects cell functions. Hence, it will be essential to reveal the impact of free DHA molecules on the domain stability and membrane potential of cell membranes.

In order to address the above issue, the three-component lipid bilayer DPPC/DUPC/CHOL (DPPC: dipalmitoyl-phosphatidylcholine, DUPC: dilinoleoyl-phosphatidylcholine, CHOL: cholesterol) and μs-scale coarse-grained molecular dynamics (MD) simulation were employed in the current work. The former has been widely used as a model system for lipid rafts to study the dynamics of lipids and proteins.[35−40] The latter is a powerful computational tool for revealing the molecular mechanisms of biological processes.[41−43] Besides, DHA molecules are generally negatively charged under physiological conditions and can also be protonated into neutral molecules with the help of certain proteins and local low pH.[44,45] Therefore, in this work, we performed a series of coarse-grained MD simulations to systematically study the effects of both anionic and neutral DHA molecules on the model cell membrane (lipid rafts). We firstly studied the self-assembly process of DHA molecules, and then the fusion process of DHA molecules with phase-separated lipid membranes. Last, a systematic analysis of the physical properties of lipid membranes was performed.

MODEL AND METHODS

Coarse-Grained Model and Simulation Details. Coarse-grained models, which allow simulations at larger length scales and longer time scales, have been widely applied for MD simulations. In this work, the Martini coarse-grained model (version 2.1)[46,47] was used to study the interactions between anionic/neutral DHA (DHA^-, DHA) molecules and the phase-separated lipid bilayer. The Martini coarse-grained model is based mainly on a four-to-one mapping rule. In other words, on average, four heavy atoms are mapped into a single interaction site. Four main types of interaction sites, including polar (P), nonpolar (N), apolar (C), and charged (Q), are used. Details can be found in the original papers of the Martini force field.[46,47] For all simulations, the cutoff of 1.2 nm was used for both van der Waals and electrostatic interactions. In order to reduce the cutoff noise, the former was smoothly shifted from 0.9 to 1.2 nm, and the latter was shifted from 0 to 1.2 nm. For computational efficiency, the MARTINI force field was parametrized towards $\varepsilon_r = 15$ for overall electrostatic interactions.[47] Hence, the default relative dielectric constant ($\varepsilon_r = 15$) was used. DHA molecules, lipids, water, and ions were coupled separately to V-rescale heat baths[48] at $T = 310$ K (coupling constant $\tau = 1$ ps). Isotropic and semi-isotropic Parrinello-Rahman pressure coupling schemes were used, respectively, for DHA self-assembly and lipid membrane simulations[49] with a compressibility of 3×10^{-4} bar^{-1} and a coupling constant (τ) of 5 ps. Each DHA self-assembly simulation and lipid membrane simulation were run for 3 and 10 μs, respectively, with a time step of 20 fs using GROMACS simulation package (version 2019.06)[50,51] and the periodic boundary condition. All system snapshots were generated by VMD.[52]

DHA Self-assembly and Lipid Membrane Simulations. In order to reveal the detailed aggregation state of DHA molecules, we performed Martini coarse-grained MD simulations to study the self-assembly details of anionic and neutral DHA molecules. In all, 16, 32 or 64 DHA^- or DHA molecules was initially evenly placed in the box with the dimensions of 13 × 13 × 19 nm^3, and solvated with water and 150 mM NaCl. Then, after a 10,000-step energy minimization and 500-ps pre-equilibration simulation, each of the six systems was run for 3 μs. The aggregation kinetics of the DHA molecules was recorded and quantified using the number of contacts between these molecules. The obtained DHA nanoclusters are named as $16DHA^-$, $32DHA^-$, $64DHA^-$, 16DHA, 32DHA, and 64DHA, respectively. In order to capture the characteristics of the cell membrane domains, we chose the three-component lipid membrane consisting of saturated DPPC, unsaturated DUPC, and CHOL in the ratio of 5:3:2.[23,35] The lipid bilayer, which contained 286 DPPC, 172 DUPC, 114 CHOL, 20552 water molecules, and 150 mM NaCl, was initially constructed using the tool *insane.py* (http://cgmartini.nl/images/tools/insane/*insane.py*).[53] The DHA nanocluster from DHA self-assembly simulations was placed close to the surface of the lipid bilayer. In order to achieve the membrane conformation where the DHA nanocluster adsorbs onto the phase-separated lipid membrane, we fixed the DHA nanocluster and ran 2 μs coarse-grained MD simulation for each of six DHA^- membrane systems at $T = 310$ K. During this 2 μs, the lipid membrane experienced obvious liquid−liquid phase separation and reached a stable state. Then, the position restraints for the DHA molecules were removed, and these six systems were further simulated for 10 μs at $T = 310$ K; the snapshots were saved in the trajectories every 10 ns to capture the detailed interactions between DHA molecules and the model cell membrane. For clarity, the corresponding membrane systems were also named as $16DHA^-$, $32DHA^-$, $64DHA^-$, 16DHA, 32DHA, and 64DHA. The pure membrane system was named as MEMB.

Trajectory Analysis. *Membrane Domain Preference of DHA and CHOL.* In order to quantify the relative localization of DHA or CHOL molecules in lipid raft and nonraft membrane domains, two kinds of analysis were performed. For one analysis, the contact ratios between DHA or CHOL molecules and DPPC/DUPC molecules are calculated using the GROMACS tool *gmx mindist*[50] with the cutoff of 0.6 nm. For the second analysis, the trajectory of the DHA head group is superimposed over the two-dimensional (2D) number-density map of DPPC molecules based on the last 500 ns of each simulation. The former is calculated using the GROMACS tool *gmx traj*,[50] and the latter is obtained by the GROMACS tool *gmx densmap*.[50] In the 2D density map, the high-density region corresponds to the lipid raft membrane domain, while the low-density region represents the lipid nonraft membrane domain.

Mass/Charge Density and Electrostatic Potential Calculation. Based on the Poisson equation,[54] the electrostatic potential $\psi(z)$ along the z-direction was calculated through the double integration of the charge density $\rho(z)$,

$$\psi(z) = -\frac{1}{\varepsilon_0 \varepsilon_r} \int_{-z}^{z} dz' \int_{-z'}^{z'} \rho(z'')dz'' \quad (1)$$

https://doi.org/10.1021/acs.jcim.2c00074
J. Chem. Inf. Model. XXXX, XXX, XXX−XXX

where ε_0 is the vacuum dielectric constant, with value 8.854×10^{-12} F·m^{-1}, and $\varepsilon_r = 15$.[47] For more precise calculation of $\rho(z)$, the in-house script was used to avoid the possible artifacts arising from the fluctuation of the box z-dimension.[29,55] In this algorithm, the center of the lipid membrane, which is defined as $z = 0$ nm, was calculated for each frame. Then, the z range $[-4, 4]$ nm was divided into 80 bins for the calculation of mass/charge density over the selected trajectory.

Evaluation of Lipid Membrane Liquid−Liquid Phase Separation. As is well known, the DPPC/DUPC/CHOL lipid membrane can have obvious liquid−liquid phase separation.[23,35] DPPC and CHOL molecules are the main components of the liquid-ordered (L_o, lipid raft) membrane domain, while the liquid-disordered (L_d, lipid nonraft) membrane domain is mainly composed of DUPC molecules. In order to evaluate the liquid−liquid phase separation process of the lipid membrane, we adopted the normalized lateral contacts between DPPC molecules. The lateral contact number between DPPC molecules of the pure DPPC bilayer with the same number of DPPC molecules is defined as the maximum for the normalization. The contact number is calculated using the GROMACS tool *gmx mindist*[50] with the cutoff of 0.6 nm.[23,24,56]

Calculation of Area Per Lipid and Membrane Thickness. In this work, the APL@Voro[57] open source program, which is compatible to GROMACS,[50] was used to calculate the area per lipid (APL) and membrane thickness. In this program, the head-group beads were firstly chosen. For the calculation of APL, these beads in each membrane leaflet were projected into the $x-y$ plane separately and then Voronoi analysis was performed. The area of each Voronoi polygon was calculated as the area of the corresponding lipid. For the calculation of membrane thickness, each bead was firstly projected into the opposite membrane leaflet to identify the nearest bead in the $x-y$ plane. Then, the z-distance between the bead and the identified nearest bead in the opposite membrane leaflet was calculated as the local membrane thickness of the lipid.

Cholesterol Preference. Cholesterol preference (χ) was calculated based on the number of contacts of cholesterol with saturated (N_1) and unsaturated lipids (N_2) as

$$\chi_1 = \frac{N_1/n_1}{N_1/n_1 + N_2/n_2},\ \chi_2 = \frac{N_2/n_2}{N_1/n_1 + N_2/n_2},$$
$$\Delta\chi = \chi_1 - \chi_2$$

where χ_1 and χ_2 are the fractional contacts of cholesterols with saturated DPPC and unsaturated DUPC lipids, and n_1 and n_2 are the total number of CG beads of saturated and unsaturated lipids, respectively. Cholesterol preference difference $\Delta\chi$ is the difference between χ_1 and χ_2.

Flip-Flop Rate of DHA and CHOL. Small molecules such as DHA and CHOL can spontaneously flip-flop between the membrane leaflets without the help of certain transporter proteins. In order to capture the flip-flop event, we chose the head group of the DHA/CHOL molecule for the analysis. The z-distance between the head group and the membrane center was recorded in real time. If the change of z-distance is larger than half of the membrane thickness, one flip-flop event was counted. Over the selected trajectory, the flip-flop rate was calculated by dividing the total flip-flop events by the time duration and number of molecules.[58]

RESULTS AND DISCUSSION

DHA Molecules Can Self-assemble into Nanoclusters, Fuse with Lipid Membranes, and Locate Mainly at the Liquid-Disordered Membrane Domain. In order to reveal the aggregation state of DHA molecules in aqueous solution, anionic/neutral DHA molecules were initially evenly distributed in the simulation box ($12 \times 12 \times 12$ nm^3) with three different concentrations. After a 10000-step energy minimization and 500-ps pre-equilibration simulation, each system went through 3 μs coarse-grained MD simulations. As shown in Figure 1 and Supporting Information, in all cases, DHA

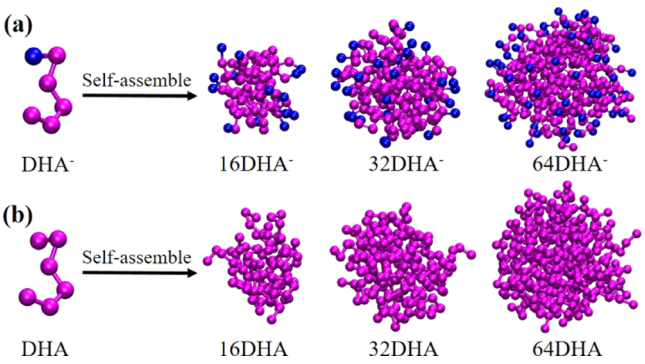

Figure 1. Snapshots for the individual DHA molecule and DHA nanoclusters of the last frame of 3 μs self-assembly simulations. DHA molecules (DHA$^-$: anionic, DHA: neutral) are colored in purple, except for the charged head group (blue) of DHA$^-$.

molecules could spontaneously self-assemble into DHA nanoclusters. The formation of DHA nanoclusters can be ascribed to the amphiphilicity of both anionic and neutral DHA molecules. However, for the case of anionic DHA molecules, the strong electrostatic repulsion among their head groups did not prevent the corresponding aggregation process. This is because this repulsive interaction was greatly relieved by cations/counterions (Na^+) in aqueous solution, which is consistent with the impact of cations (e.g., Ca^{2+}) on the clustering of anionic membrane lipids such as polyphosphoinositides.[59] Since DHA molecules can self-assemble into spherical nanoclusters, we focus on their subsequent interactions with the model cell membrane.

We then placed the DNA nanoclusters tightly close to the surface of the lipid membrane to reveal the molecular details for their fusion with the lipid membrane. These DHA-membrane systems were generated using *insane.py*.[53] First, each system was run for 2 μs coarse-grained MD simulations with the DHA nanocluster being fixed. During this period, we could witness the clear phase separation of the lipid membrane (Supporting Information), which is consistent with the time scale of previous simulations.[35] Then, the constraints on the DHA nanocluster were removed and each system was further run for another 10 μs to capture the whole fusion process. As shown in Figure 2 and Supporting Information, all DHA nanoclusters could fuse with the lipid membrane and DHA molecules fully dispersed in the membrane. The fused DHA molecules could then flip-flop between the two membrane leaflets to achieve the approximately equal distribution in two membrane leaflets (Supporting Information). Generally, increasing the nanocluster size slightly increases the difficulty of the membrane fusion, while the ionization of DHA head groups can promote the membrane fusion. Consistent with the

https://doi.org/10.1021/acs.jcim.2c00074
J. Chem. Inf. Model. XXXX, XXX, XXX−XXX

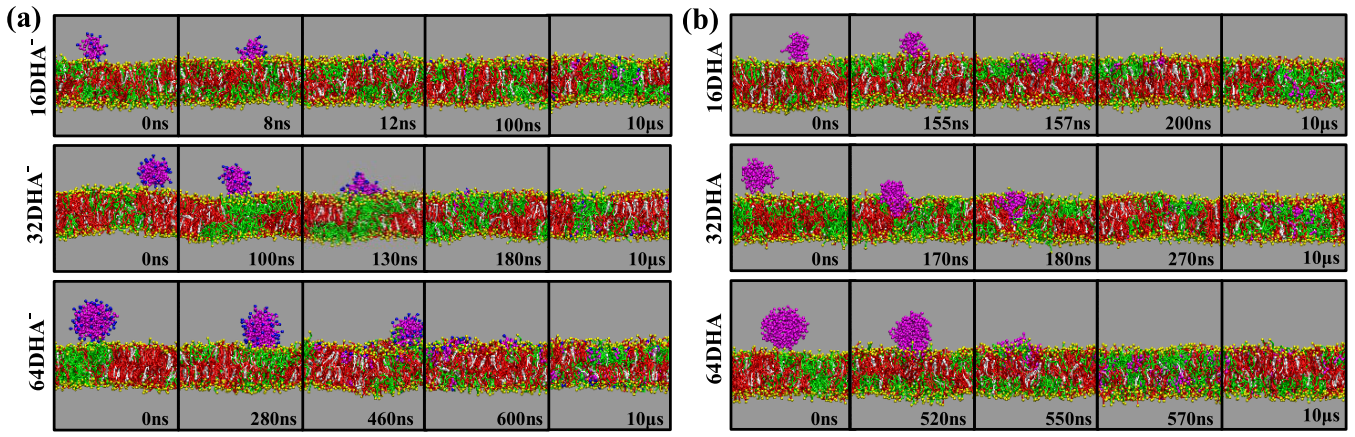

Figure 2. Side-view system snapshots of the fusion processes of anionic (a) and neutral (b) DHA molecules with the lipid membrane. The coloring style of DHA is the same as Figure 1. DPPC and DUPC are colored in red and green, while their head groups are colored in yellow. CHOL was colored in white. Ions and water molecules are not shown for clarity.

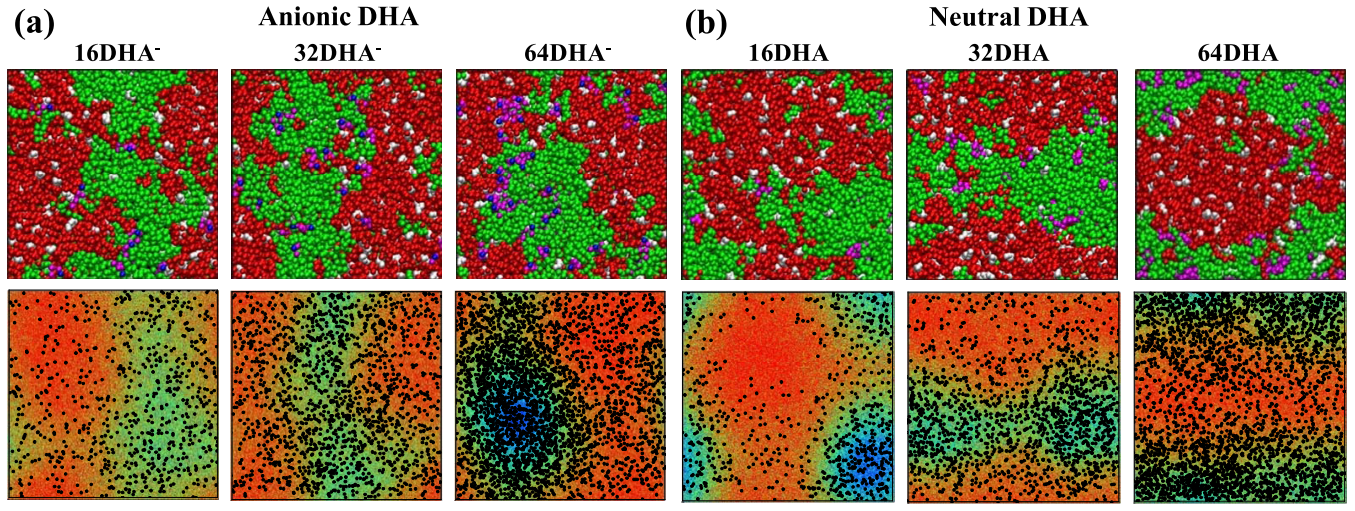

Figure 3. DHA molecules prefer to locate at the L_d membrane domains of DPPC/DUPC/CHOL bilayers. Top-view system snapshots (t = 10 μs, upper panel) and 2D DPPC number-density maps (lower panel) of membrane systems with anionic (a) and neutral (b) DHA molecules. The coloring style for the snapshots is the same as in Figure 2. In the number-density map, which is averaged over the last 500 ns of each trajectory, the density of DPPC molecules decreases from red to blue. Each black point represents the position of one DHA molecule.

size effect of nanoparticles in crossing the lipid bilayer,[60,61] the increase in DHA nanocluster size will increase the energy barrier to penetrate into the lipid membrane and thus the difficulty of the membrane fusion. Hence, it will take more time to have the complete membrane fusion. The ionization of DHA head groups promotes the electrostatic interactions between the negative DHA head group and positive trimethyl ammonium in lipid head groups. These enhanced electrostatic interactions thus promote the membrane fusion.

We further analyzed the membrane domain preference of DHA molecules within the phase-separated lipid bilayers using system snapshots and DPPC number density over the last 500 ns of each 10 μs trajectory. As shown in Figure 3, both the anionic and neutral DHA molecules preferred to locate at the L_d membrane domains. Considering the general differences in the lipid unsaturation and the cholesterol ratio between L_o and L_d membrane domains,[17,23,62] this preference is expected for the polyunsaturated fatty acids (e.g., DHA[63]) or lipid anchor (e.g., farnesylation[28,64]). It is worth mentioning that these small and flexible DHA molecules have strong lateral diffusion ability. They can also access the L_o membrane domain, especially when the DHA concentration is high (Figure 3, 64DHA$^-$ and 64DHA).

Anionic DHA Molecules Dramatically Reshape the Intrinsic Transmembrane Potential of the Lipid Membrane during the Fusion Process. In this work, we used the PMEPOT plug-in[65] of VMD[52] to capture the whole electrostatic potential (ψ) maps of the simulation systems and the changes during the membrane fusion process of DHA molecules (Figure 2). As shown in Figure 4, our ψ map indicated that the potential of the region outside the lipid membrane generally was larger than that of the membrane interior, which is consistent with the ψ profile across symmetric lipid membranes calculated using the Poisson equation based on the coarse-grained MD simulations.[66,67] Also, in atomistic membrane systems, PMEPOT showed consistent results of V_m with the calculation based on the Poisson equation.[68] Hence, PMEPOT is a reliable tool to capture the detailed impact of DHA nanoclusters on the ψ maps of membrane systems. It is worth mentioning that the overall $\psi(z)$ profiles across the lipid membrane may be significantly different among different force fields due to

https://doi.org/10.1021/acs.jcim.2c00074
J. Chem. Inf. Model. XXXX, XXX, XXX−XXX

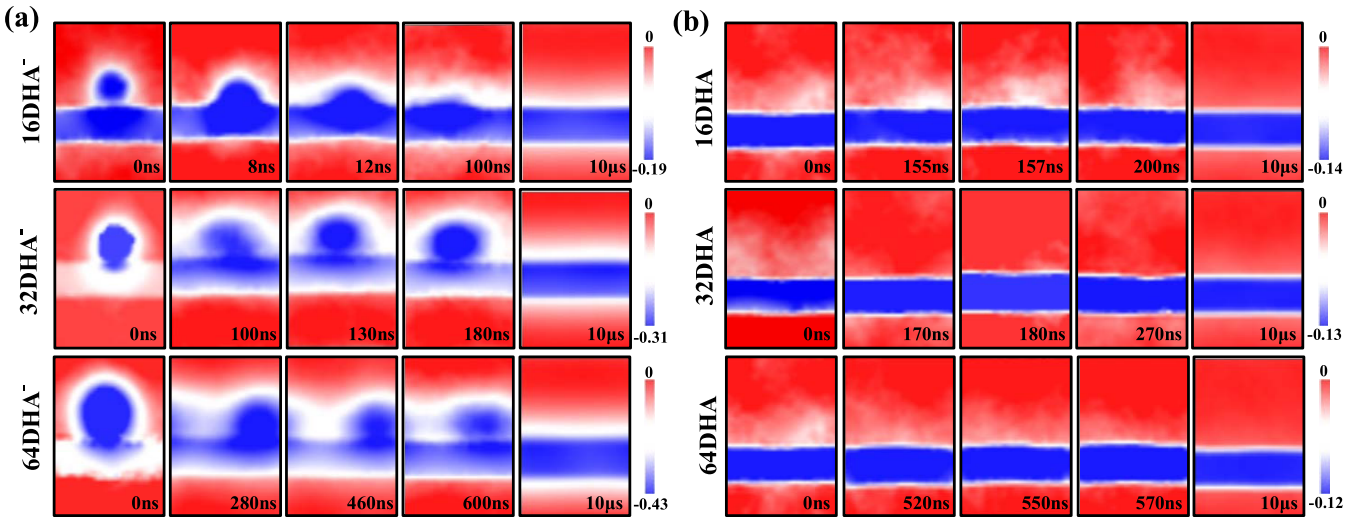

Figure 4. 2D ψ maps of membrane systems with anionic (a) and neutral (b) DHA molecules corresponding to the snapshots shown in Figure 2. The unit for the color bar is volt (V). In order to maximize the visualization for the differences of electrostatic potential at different regions, different ranges of color bar were used for different systems.

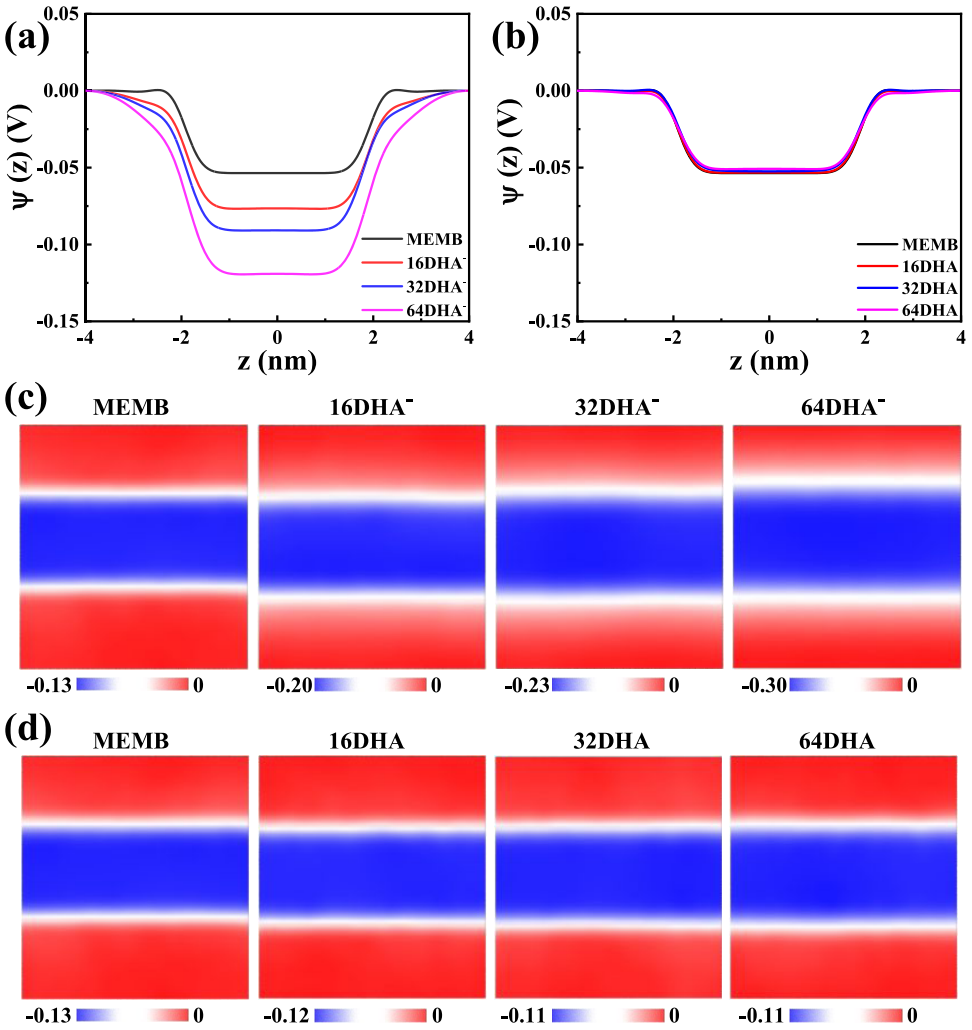

Figure 5. ψ profiles (a, b) and maps (c, d) across the lipid bilayers with anionic (a, c) or neutral (b, d) DHA molecules. The unit for the color bar is volt (V). In order to maximize the visualization for the differences of electrostatic potential at different regions, different ranges of color bar were used for different systems.

https://doi.org/10.1021/acs.jcim.2c00074
J. Chem. Inf. Model. XXXX, XXX, XXX−XXX

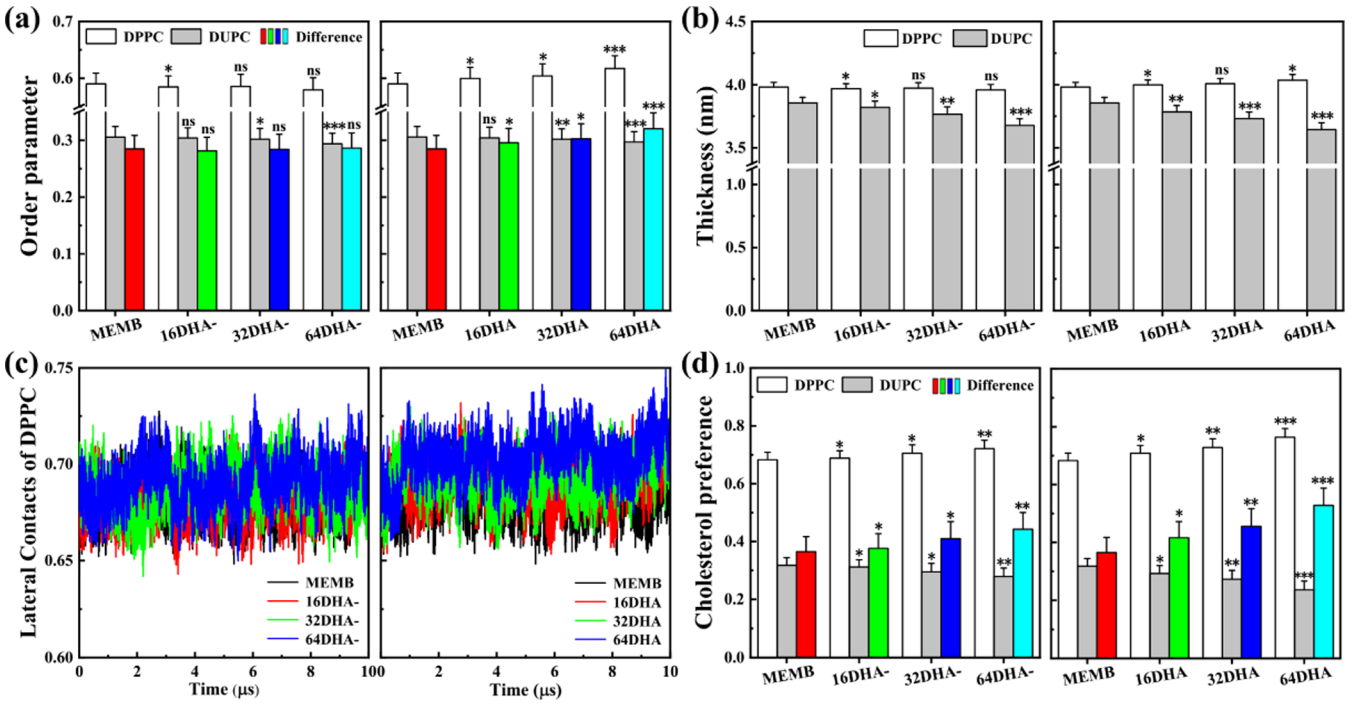

Figure 6. Effects of DHA molecules (left panel: anionic DHA, right panel: neutral DHA) on the physical properties of the DPPC/DUPC/CHOL phase-separated lipid membrane: (a) lipid chain order parameter, (b) membrane thickness, (c) time evolution of normalized lateral contacts between saturated lipids (DPPC), and (d) cholesterol preference differences. Mean ± SD was calculated using the block average over the last 6 μs of each 10 μs trajectory (3 blocks: 4−6, 6−8, 8−10 μs). Statistical significance was obtained by Student's t-test with system MEMB as the control. $^{*}p < 0.05$, $^{**}p < 0.01$, $^{***}p < 0.001$.

different resolutions and partial charge assignments. For example, electrostatic potential profiles $\psi(z)$ differ much especially in the membrane interior region among membrane systems using coarse-grained,[66,67] atomistic,[29,54,55] and polarizable force fields.[69] However, previous studies have indicated that the MARTINI force field generally could reproduce the effects of the constant electric field[66,70] and charged nanoparticles/biomolecules[67] on the transmembrane potential differences (V_m) of model cell membranes. Hence, it is feasible to probe the effects of DHA nanoclusters on the V_m of the model cell membrane using the MARTINI force field.

Comparing the ψ maps between membrane systems with anionic and neutral DHA nanoclusters, we could find that neutral DHA nanoclusters had much more moderate effects on the ψ map of the membrane. For the neutral DHA nanocluster, when it adhered to the lipid membrane, this nanoscale micelle of amphiphilic DHA molecules had a relatively low ψ, which affected the overall ψ map or V_m most at this moment. However, along with the membrane fusion process of the neutral DHA nanocluster, the disturbance on the overall ψ map or V_m gradually disappeared (Figure 4b). As for the anionic DHA nanocluster, the impact was much more significant. This could be ascribed to the negative charges of the DHA head groups, which induced ultra-low interior ψ of the DHA nanocluster (Figure 4a). In other words, a larger anionic DHA nanocluster carries more negative charges, and thus has a more significant impact on the V_m, which explained the nanocluster size-dependent impact (Figure 4a). In both cases, after the complete fusion of DHA nanoclusters with the lipid membrane and sufficient equilibrium simulations (flip-flop of DHA and CHOL), the overall $\psi(z)$ distribution across the lipid membrane became symmetric (t = 10 μs), which was expected for the symmetric membrane systems. However, unlike the neutral DHA molecules, anionic DHA molecules greatly increased the electrostatic potential difference ($\Delta\psi$) between the lipid membrane surface and interior.

As discussed above, DHA molecules were mainly distributed in the L_d membrane domain. In order to further confirm the impact of DHA nanoclusters on the intrinsic membrane potential of the three-component model cell membrane (Figure 4), we further studied the pure DUPC lipid bilayer (MEMB) as well as symmetric DUPC/DHA lipid bilayers (16, 32, and 64 DHA^-/DHA). A 4-μs coarse-grained MD simulation was performed at body temperature for each system. We performed ψ analysis for these systems using both the double integration of the Poisson equation[54,66] and PMEPOT[65] over the last 500 ns of each trajectory. As shown in Figure 5, the ψ profiles and maps were consistent with each other, both of which strongly indicated that anionic DHA molecules significantly reshaped the ψ profile or map across the lipid membrane and their impact is concentration-dependent (Figure 5a,c). The electrostatic potential difference ($\Delta\psi$) between the inside and outside of the lipid membrane was highly sensitive to the ratio of anionic DHA molecules. As for the neutral DHA molecules, the situation is dramatically different. Almost no significant impact on the overall $\psi(z)$ profiles of the lipid membrane could be found for all of the tested concentrations (Figure 5b,d).

Incorporation of DHA Molecules Changes the Structural and Dynamical Properties of the Phase-Separated Lipid Membranes. As discussed above, DHA molecules could fuse with the lipid membrane, locate preferably at the L_d membrane domain, and reshape ψ profiles or maps across the lipid membrane, which thus may regulate a series of transmembrane potential V_m-involving biological processes such as cell proliferation and differentiation.[71] This

https://doi.org/10.1021/acs.jcim.2c00074
J. Chem. Inf. Model. XXXX, XXX, XXX−XXX

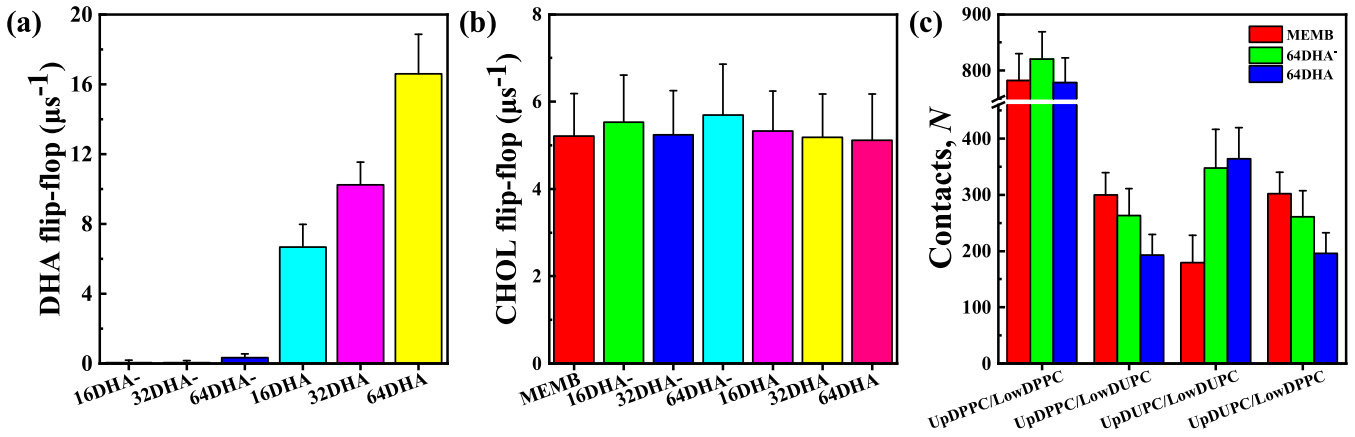

Figure 7. Effects of DHA molecules on *interleaflet* couplings and dynamics of DPPC/DUPC/CHOL phase-separated lipid membrane. (a) Flip-flop rates of DHA molecules. (b) Flip-flop rates of CHOL molecules. (c) Interleaflet contacts of DPPC and DUPC molecules. Mean ± SD was calculated using the block average over the last 6 μs of each 10 μs trajectory (3 blocks: 4−6, 6−8, 8−10 μs).

explained why feeding the cell with DHA molecules could change the cell proliferation and differentiation.[72] In order to reveal other possible effects of DHA molecules on the plasma membrane, we further analyzed the structural and dynamical properties of the lipid membrane domains. As shown in Figure 6, the incorporation of DHA molecules into the lipid membrane could slightly increase the lipid chain order parameter (Figure 6a) and thickness (Figure 6b) of the L_o membrane domain and decrease the corresponding structural parameters of the L_d membrane domain. Especially, neutral DHA is more obvious. In other words, the differences of lipid chain order and membrane thickness between L_o and L_d membrane domains and thus the stability of the membrane domain intraleaflet dynamics (Figure 6c) were enhanced by DHA molecules. The enhancement depended on the ratio of DHA molecules. Since the highly flexible DHA molecules are mainly located in the L_d membrane domain, they could make the lipids of the L_d membrane domain more disordered.[73−75] This could be ascribed to the high unsaturation and thus high flexibility of DHA molecules, which is consistent with previous studies on the formation of membrane domains.[23,35] However, the reason for the enhanced lipid chain order of the L_o membrane domain is still unclear. Hence, we further analyzed the cholesterol preference for L_o and L_d membrane domain lipids (DPPC and DUPC). As shown in Figure 6d, we could find that the incorporation of DHA molecules into the L_d membrane domain could promote the cholesterol preference to L_o membrane domain lipids. That is, DHA molecules did not prefer to interact with the cholesterol molecules and thus drove cholesterol molecules into the L_o membrane domain, which is consistent with previous research studies on the roles of polyunsaturated fatty acids in the membrane domain formation[76] and explains the structural changes in the L_o membrane domain mentioned above.

The above analysis revealed the overall changes of the structural properties induced by DHA molecules, which are essential for the stability of membrane domain intraleaflet dynamics. As is known, in addition to this intraleaflet membrane domain dynamics, the interleaflet membrane domain dynamics is another essential part of lipid raft dynamics.[24,25] Also, previous studies have demonstrated that factors such as the lipid (e.g., cholesterol) exchange[56,77,78] between the two membrane leaflets will be essential for the interleaflet coupling strength, which determines the interleaflet membrane domain dynamics. Hence, we analyzed the lipid flip-flop events and quantified the degree of membrane domain registration/antiregistration in our simulation systems. Our results indicated that DHA molecules could flip-flop between the two membrane leaflets similar to CHOL molecules, which is consistent with previous atomistic studies showing that DHA can flip-flop in the model of the human brain cell membrane.[74] In addition, the head-group ionization greatly impeded the flip-flop processes of DHA molecules (Figure 7a), which are concentration-dependent. For amphiphilic molecules such as CHOL molecules, the flip-flop process is mainly determined by the energy barrier at the membrane hydrophobic center, which depends on the hydrophilicity of amphiphilic molecules.[79] Compared to the neutral DHA molecules, the anionic DHA molecules have much higher polar head groups (hydrophilicity), which greatly increases the energy barrier required to cross the membrane hydrophobic center and thus induces much lower flip-flop rates. In addition, it is reported that DHA can partially reverse the effect of CHOL on the lipid bilayer, making the membrane more compressible and fluid.[75] Also, in our work, we found that the presence of DHA molecules also had slight effects on the CHOL flip-flop (Figure 7b). Especially, anionic DHA molecules could promote the CHOL flip-flop rate to a certain degree. Both the flip-flop processes of DHA and CHOL molecules play key roles in the lipid exchange and thus the coupling strength between the two membrane leaflets, which determines the interleaflet dynamics of membrane domains.[24,56,77,78] Considering the main components of L_o and L_d membrane domains as DPPC and DUPC molecules, we therefore calculated the interleaflet contacts between them to quantify the effects of DHA molecules on the aforementioned interleaflet dynamics (domain registration/antiregistration). As shown in Figure 7c, with the presence of anionic/neutral DHA molecules mainly in the L_d domain, the contacts between the upper and lower DUPC molecules were greatly enhanced and neutral DHA molecules became more significant. Meanwhile, the interleaflet contacts between DPPC and DUPC molecules were reduced. This indicated that DHA molecules could regulate the interleaflet dynamics of membrane domains and promote the membrane domain registration.

https://doi.org/10.1021/acs.jcim.2c00074
J. Chem. Inf. Model. XXXX, XXX, XXX−XXX

Scheme 1. DNA Molecules Can Fuse with the Lipid Membrane and Regulate Its Membrane Potential as well as Membrane Domain Dynamics

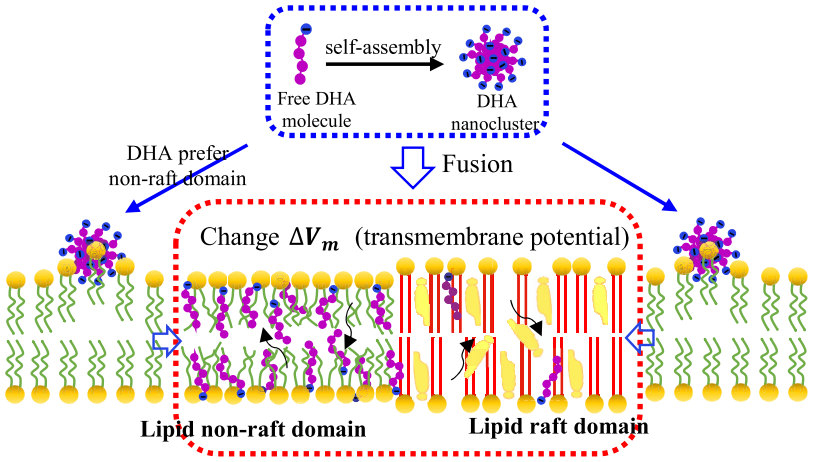

CONCLUSIONS

In this work, through a series of μs-scale coarse-grained MD simulations, our results showed that both anionic and neutral DHA molecules can spontaneously self-assemble into nanoclusters, fuse with the lipid membrane, and mainly locate in the L_d membrane domain (Scheme 1). The head-group ionization of DHA molecules enhanced the membrane fusion process and greatly reshaped the transmembrane potential of the lipid membrane. On the other hand, the enrichment of DHA molecules in the L_d membrane domain and their own flip-flop dynamics could further affect the preferred localization and flip-flop of CHOL molecules, which in turn modulated the intraleaflet and interleaflet membrane domain dynamics. After DHA incorporation, the differences in lipid chain order, cholesterol preference, and membrane thickness between L_o and L_d membrane domains are enhanced, which promote the stability of the membrane domain intraleaflet dynamics. The flip-flop of both DHA and CHOL molecules as well as the change in lipid chain order jointly regulate the interleaflet coupling and thus promote membrane domain registration. Besides, most effects induced by DHA molecules showed a concentration-dependent manner. In short, the detailed molecular-level impact of free DHA molecules on the physical properties of the model cell membrane revealed in this work will provide useful insights for understanding the physiological functions of DHA molecules and developing therapeutics for diseases due to DHA deficiency.

ASSOCIATED CONTENT

Supporting Information

The Supporting Information is available free of charge at https://pubs.acs.org/doi/10.1021/acs.jcim.2c00074.

Coarse-grained mapping of DHA molecules, snapshots and DHA−DHA contacts for self-assembly simulations, snapshots for phase separation simulations, time evolution of distances between DHA nanoclusters with lipid membrane during the membrane fusion processes, mass density profiles of different concentration of anionic and neutral DHA, charge density profiles of the anionic and neutral DHA/DUPC lipid membrane, time evolution of area per lipid (APL) and thickness of lipid bilayers. Movies for the flip-flop of DHA and CHOL molecules as well as the control simulation with the PME treatment (PDF)

Movie for highlighting the flip-flop of DHA and CHOL molecules based on 9−10 μs of system 16DHA. The upper and lower leaflet of the lipid membrane are colored in white and gray. DHA and CHOL molecules are colored in purple and yellow beads (MPG)

Movie for highlighting the flip-flop of DHA and CHOL molecules based on 9−10 μs of system 16DHA$^-$. The upper and lower leaflet of the lipid membrane are colored in white and gray. DHA and CHOL molecules are colored in purple and yellow beads (MPG)

Movie for the first 2 μs of 5 μs MD simulations of system 16DHA$^-$ with the PME treatment for electrostatic interactions (MPG)

AUTHOR INFORMATION

Corresponding Author

Xubo Lin − *Beijing Advanced Innovation Center for Biomedical Engineering, School of Engineering Medicine & School of Biological Science and Medical Engineering, Beihang University, Beijing 100191, China;* orcid.org/0000-0002-4417-3582; Email: linxbseu@buaa.edu.cn

Authors

Xiu Li − *Beijing Advanced Innovation Center for Biomedical Engineering, School of Engineering Medicine & School of Biological Science and Medical Engineering, Beihang University, Beijing 100191, China*

Shiying Zhou − *Beijing Advanced Innovation Center for Biomedical Engineering, School of Engineering Medicine & School of Biological Science and Medical Engineering, Beihang University, Beijing 100191, China*

Complete contact information is available at: https://pubs.acs.org/10.1021/acs.jcim.2c00074

Author Contributions

Conceptualization: X.B.L.; methodology: X.B.L., X.L., S.Y.Z.; formal analysis: X.L., X.B.L., S.Y.Z.; investigation and visualization: X.L., X.B.L., S.Y.Z.; writing-original draft: X.L.; writing-review and editing: X.B.L.; funding acquisition: X.B.L.; project administration: X.B.L. All authors have read and agreed to the published version of the manuscript.

https://doi.org/10.1021/acs.jcim.2c00074
J. Chem. Inf. Model. XXXX, XXX, XXX−XXX

Notes

The authors declare no competing financial interest.

Data: the Martini force field parameters for lipids, water and ions as well as the scripts including *insane.py* can be freely accessed from the official website of the force field (http://cgmartini.nl/). The molecular dynamics trajectories can be obtained from the corresponding author upon request. Software: GROMACS 2019.6 (http://www.gromacs.org/), gnuplot 5.2 (http://www.gnuplot.info/), and VMD 1.9.3 (http://www.ks.uiuc.edu/Research/vmd/) used in this work can be downloaded free of charge from their official websites.

■ ACKNOWLEDGMENTS

This work was supported by the National Natural Science Foundation of China (No. 21903002), the Fundamental Research Funds for the Central Universities (No. YWF-20-BJ-J-632), the Open Fund of State Key Laboratory of Membrane Biology (No. 2020KF09). We are grateful to Center for High Performance Computing of Beihang University (BHHPC) for generous computing resources.

■ REFERENCES

(1) Harris, W. S.; Miller, M.; Tighe, A. P.; Davidson, M. H.; Schaefer, E. J. Omega-3 Fatty Acids and Coronary Heart Disease Risk: Clinical and Mechanistic Perspectives. *Atherosclerosis* **2008**, *197*, 12−24.

(2) Jones, P. J. S.; Senanayake, V. K.; Pu, S.; Jenkins, D. J. A.; Connelly, P. W.; Lamarche, B.; Couture, P.; Charest, A.; Baril-Gravel, L.; West, S. G.; Liu, X.; Fleming, J. A.; McCrea, C. E.; Kris-Etherton, P. M. Dha-Enriched High-Oleic Acid Canola Oil Improves Lipid Profile and Lowers Predicted Cardiovascular Disease Risk in the Canola Oil Multicenter Randomized Controlled Trial. *Am. J. Clin. Nutr.* **2014**, *100*, 88−97.

(3) Miles, E. A.; Childs, C. E.; Calder, P. C. Long-Chain Polyunsaturated Fatty Acids (Lcpufas) and the Developing Immune System: A Narrative Review. *Nutrients* **2021**, *13*, No. 247.

(4) Talamonti, E.; Sasso, V.; To, H.; Haslam, R. P.; Napier, J. A.; Ulfhake, B.; Pernold, K.; Asadi, A.; Hessa, T.; Jacobsson, A.; Chiurchiù, V.; Viscomi, M. T. Impairment of Dha Synthesis Alters the Expression of Neuronal Plasticity Markers and the Brain Inflammatory Status in Mice. *FASEB J.* **2020**, *34*, 2024−2040.

(5) Uauy, R.; Dangour, A. D. Nutrition in Brain Development and Aging: Role of Essential Fatty Acids. *Nutr. Rev.* **2006**, *64*, S24−S33.

(6) Lauritzen, L.; Brambilla, P.; Mazzocchi, A.; Harsløf, L.; Ciappolino, V.; Agostoni, C. Dha Effects in Brain Development and Function. *Nutrients* **2016**, *8*, No. 6.

(7) Hashimoto, M.; Hossain, S.; Al Mamun, A.; Matsuzaki, K.; Arai, H. Docosahexaenoic Acid: One Molecule Diverse Functions. *Crit. Rev. Biotechnol.* **2017**, *37*, 579−597.

(8) Gorjão, R.; Azevedo-Martins, A. K.; Rodrigues, H. G.; Abdulkader, F.; Arcisio-Miranda, M.; Procopio, J.; Curi, R. Comparative Effects of Dha and Epa on Cell Function. *Pharmacol. Ther.* **2009**, *122*, 56−64.

(9) Yang, B.; Fritsche, K. L.; Beversdorf, D. Q.; Gu, Z.; Lee, J. C.; Folk, W. R.; Greenlief, C. M.; Sun, G. Y. Yin-Yang Mechanisms Regulating Lipid Peroxidation of Docosahexaenoic Acid and Arachidonic Acid in the Central Nervous System. *Front. Neurol.* **2019**, *10*, No. 642.

(10) Levental, K. R.; Lorent, J. H.; Lin, X.; Skinkle, A. D.; Surma, M. A.; Stockenbojer, E. A.; Gorfe, A. A.; Levental, I. Polyunsaturated Lipids Regulate Membrane Domain Stability by Tuning Membrane Order. *Biophys. J.* **2016**, *110*, 1800−1810.

(11) Huber, T.; Rajamoorthi, K.; Kurze, V. F.; Beyer, K.; Brown, M. F. Structure of Docosahexaenoic Acid-Containing Phospholipid Bilayers as Studied by ^{2}H Nmr and Molecular Dynamics Simulations. *J. Am. Chem. Soc.* **2002**, *124*, 298−309.

(12) Wassall, S. R.; Leng, X.; Canner, S. W.; Pennington, E. R.; Kinnun, J. J.; Cavazos, A. T.; Dadoo, S.; Johnson, D.; Heberle, F. A.; Katsaras, J.; Shaikh, S. R. Docosahexaenoic Acid Regulates the Formation of Lipid Rafts: A Unified View from Experiment and Simulation. *Biochim. Biophys. Acta* **2018**, *1860*, 1985−1993.

(13) Hoshi, T.; Wissuwa, B.; Tian, Y.; Tajima, N.; Xu, R.; Bauer, M.; Heinemann, S. H.; Hou, S. Omega-3 Fatty Acids Lower Blood Pressure by Directly Activating Large-Conductance Ca2+-Dependent K+ Channels. *Proc. Natl. Acad. Sci.* **2013**, *110*, 4816−4821.

(14) Newell, M.; Baker, K.; Postovit, L. M.; Field, C. J. A Critical Review on the Effect of Docosahexaenoic Acid (Dha) on Cancer Cell Cycle Progression. *Int. J. Mol. Sci.* **2017**, *18*, No. 1784.

(15) Sampaio, J. L.; Gerl, M. J.; Klose, C.; Ejsing, C. S.; Beug, H.; Simons, K.; Shevchenko, A. Membrane Lipidome of an Epithelial Cell Line. *Proc. Natl. Acad. Sci.* **2011**, *108*, 1903−1907.

(16) Klose, C.; Surma, M. A.; Simons, K. Organellar Lipidomics-Background and Perspectives. *Curr. Opin. Cell Biol.* **2013**, *25*, 406−413.

(17) Sezgin, E.; Levental, I.; Mayor, S.; Eggeling, C. The Mystery of Membrane Organization: Composition, Regulation and Roles of Lipid Rafts. *Nat. Rev. Mol. Cell Biol.* **2017**, *18*, No. 361.

(18) van Meer, G.; Voelker, D. R.; Feigenson, G. W. Membrane Lipids: Where They Are and How They Behave. *Nat. Rev. Mol. Cell Biol.* **2008**, *9*, 112−124.

(19) Lingwood, D.; Simons, K. Lipid Rafts as a Membrane-Organizing Principle. *Science* **2010**, *327*, 46−50.

(20) Lee, I.-H.; Saha, S.; Polley, A.; Huang, H.; Mayor, S.; Rao, M.; Groves, J. T. Live Cell Plasma Membranes Do Not Exhibit a Miscibility Phase Transition over a Wide Range of Temperatures. *J. Phys. Chem. B* **2015**, *119*, 4450−4459.

(21) Levental, I.; Levental, K. R.; Heberle, F. A. Lipid Rafts: Controversies Resolved, Mysteries Remain. *Trends Cell Biol.* **2020**, *30*, 341−353.

(22) Cebecauer, M.; Amaro, M.; Jurkiewicz, P.; Sarmento, M. J.; Šachl, R.; Cwiklik, L.; Hof, M. Membrane Lipid Nanodomains. *Chem. Rev.* **2018**, *118*, 11259−11297.

(23) Lin, X.; Lorent, J. H.; Skinkle, A. D.; Levental, K. R.; Waxham, M. N.; Gorfe, A. A.; Levental, I. Domain Stability in Biomimetic Membranes Driven by Lipid Polyunsaturation. *J. Phys. Chem. B* **2016**, *120*, 11930−11941.

(24) Zhang, S.; Lin, X. Lipid Acyl Chain Cis Double Bond Position Modulates Membrane Domain Registration/Anti-Registration. *J. Am. Chem. Soc.* **2019**, *141*, 15884−15890.

(25) Raghupathy, R.; Anilkumar, A. A.; Polley, A.; Singh, P. P.; Yadav, M.; Johnson, C.; Suryawanshi, S.; Saikam, V.; Sawant, S. D.; Panda, A.; Guo, Z.; Vishwakarma, R. A.; Rao, M.; Mayor, S. Transbilayer Lipid Interactions Mediate Nanoclustering of Lipid-Anchored Proteins. *Cell* **2015**, *161*, 581−594.

(26) Lin, X.; Li, Z.; Gorfe, A. A. Reversible Effects of Peptide Concentration and Lipid Composition on H-Ras Lipid Anchor Clustering. *Biophys. J.* **2015**, *109*, 2467−2470.

(27) Li, Z.; Janosi, L.; Gorfe, A. A. Formation and Domain Partitioning of H-Ras Peptide Nanoclusters: Effects of Peptide Concentration and Lipid Composition. *J. Am. Chem. Soc.* **2012**, *134*, 17278−17285.

(28) Janosi, L.; Li, Z.; Hancock, J. F.; Gorfe, A. A. Organization, Dynamics, and Segregation of Ras Nanoclusters in Membrane Domains. *Proc. Natl. Acad. Sci.* **2012**, *109*, 8097−8102.

(29) Lin, X.; Gorfe, A. A. Transmembrane Potential of Physiologically Relevant Model Membranes: Effects of Membrane Asymmetry. *J. Chem. Phys.* **2020**, *153*, No. 105103.

(30) Zhou, Y.; Wong, C. O.; Cho, Kj.; Van Der Hoeven, D.; Liang, H.; Thakur, D. P.; Luo, J.; Babic, M.; Zinsmaier, K. E.; Zhu, M. X.; Hu, H.; Venkatachalam, K.; Hancock, J. F. Membrane Potential Modulates Plasma Membrane Phospholipid Dynamics and K-Ras Signaling. *Science* **2015**, *349*, 873−876.

(31) Sundelacruz, S.; Levin, M.; Kaplan, D. L. Role of Membrane Potential in the Regulation of Cell Proliferation and Differentiation. *Stem Cell Rev.* **2009**, *5*, 231−246.

https://doi.org/10.1021/acs.jcim.2c00074
J. Chem. Inf. Model. XXXX, XXX, XXX−XXX

(32) Blackiston, D. J.; McLaughlin, K. A.; Levin, M. Bioelectric Controls of Cell Proliferation: Ion Channels, Membrane Voltage and the Cell Cycle. *Cell Cycle* **2009**, *8*, 3527−3536.
(33) Monteith, G. R.; McAndrew, D.; Faddy, H. M.; Roberts-Thomson, S. J. Calcium and Cancer: Targeting Ca^{2+} Transport. *Nat. Rev. Cancer* **2007**, *7*, 519−530.
(34) Prevarskaya, N.; Skryma, R.; Shuba, Y. Ion Channels and the Hallmarks of Cancer. *Trends Mol. Med.* **2010**, *16*, 107−121.
(35) Risselada, H. J.; Marrink, S. J. The Molecular Face of Lipid Rafts in Model Membranes. *Proc. Natl. Acad. Sci.* **2008**, *105*, 17367−17372.
(36) Marrink, S. J.; Corradi, V.; Souza, P. C. T.; Ingólfsson, H. I.; Tieleman, D. P.; Sansom, M. S. P. Computational Modeling of Realistic Cell Membranes. *Chem. Rev.* **2019**, *119*, 6184−6226.
(37) Fowler, P. W.; Williamson, J. J.; Sansom, M. S. P.; Olmsted, P. D. Roles of Interleaflet Coupling and Hydrophobic Mismatch in Lipid Membrane Phase-Separation Kinetics. *J. Am. Chem. Soc.* **2016**, *138*, 11633−11642.
(38) Rascol, E.; Devoisselle, J. M.; Chopineau, J. The Relevance of Membrane Models to Understand Nanoparticles-Cell Membrane Interactions. *Nanoscale* **2016**, *8*, 4780−4798.
(39) Moss Iii, F. R.; Cabrera, G. E.; McKenna, G. M.; Salerno, G. J.; Shuken, S. R.; Landry, M. L.; Weiss, T. M.; Burns, N. Z.; Boxer, S. G. Halogenation-Dependent Effects of the Chlorosulfolipids of Ochromonas Danica on Lipid Bilayers. *ACS Chem. Biol.* **2020**, *15*, 2986−2995.
(40) Wong, J. J.; Chen, Z.; Chung, J. K.; Groves, J. T.; Jardetzky, T. S. Ephrinb2 Clustering by Nipah Virus G Is Required to Activate and Trap F Intermediates at Supported Lipid Bilayer-Cell Interfaces. *Sci. Adv.* **2021**, *7*, No. eabe1235.
(41) Kong, X.; Xing, E.; Zhuang, T.; Li, P.-K.; Cheng, X. Mechanistic Insights into the Allosteric Inhibition of Androgen Receptors by Binding Function 3 Antagonists from an Integrated Molecular Modeling Study. *J. Chem. Inf. Model.* **2021**, *61*, 3477−3494.
(42) Weng, J.; Yang, M.; Wang, W.; Xu, X.; Tian, Z. Revealing Thermodynamics and Kinetics of Lipid Self-Assembly by Markov State Model Analysis. *J. Am. Chem. Soc.* **2020**, *142*, 21344−21352.
(43) Deng, Z.; You, X.; Yuan, B.; Yang, K. Computational Design of a Minimal "Protein-Like" Conjugate for Potent Membrane Poration. *Giant* **2021**, *8*, No. 100071.
(44) Bruno, M. J.; Rusinova, R.; Gleason, N. J.; Koeppe Ii, R. E.; Andersen, O. S. Interactions of Drugs and Amphiphiles with Membranes: Modulation of Lipid Bilayer Elastic Properties by Changes in Acyl Chain Unsaturation and Protonation. *Faraday Discuss.* **2013**, *161*, 461−480.
(45) Larsson, J. E.; Larsson, H. P.; Liin, S. I. Kcne1 Tunes the Sensitivity of Kv7.1 to Polyunsaturated Fatty Acids by Moving Turret Residues Close to the Binding Site. *eLife* **2018**, *7*, No. e37257.
(46) Marrink, S. J.; De Vries, A. H.; Mark, A. E. Coarse Grained Model for Semiquantitative Lipid Simulations. *J. Phys. Chem. B* **2004**, *108*, 750−760.
(47) Marrink, S. J.; Risselada, H. J.; Yefimov, S.; Tieleman, D. P.; De Vries, A. H. The Martini Force Field: Coarse Grained Model for Biomolecular Simulations. *J. Phys. Chem. B* **2007**, *111*, 7812−7824.
(48) Bussi, G.; Donadio, D.; Parrinello, M. Canonical Sampling through Velocity Rescaling. *J. Chem. Phys.* **2007**, *126*, No. 014101.
(49) Parrinello, M.; Rahman, A. Polymorphic Transitions in Single Crystals: A New Molecular Dynamics Method. *J. Appl. Phys.* **1981**, *52*, 7182−7190.
(50) Abraham, M. J.; Murtola, T.; Schulz, R.; Páll, S.; Smith, J. C.; Hess, B.; Lindahl, E. Gromacs: High Performance Molecular Simulations through Multi-Level Parallelism from Laptops to Supercomputers. *SoftwareX* **2015**, *1−2*, 19−25.
(51) Li, L.; Davande, H.; Bedrov, D.; Smith, G. D. A Molecular Dynamics Simulation Study of C60 Fullerenes inside a Dimyristoylphosphatidylcholine Lipid Bilayer. *J. Phys. Chem. B* **2007**, *111*, 4067−4072.
(52) Humphrey, W.; Dalke, A.; Schulten, K. Vmd: Visual Molecular Dynamics. *J. Mol. Graphics* **1996**, *14*, 33−38.
(53) Wassenaar, T. A.; Ingólfsson, H. I.; Böckmann, R. A.; Tieleman, D. P.; Marrink, S. J. Computational Lipidomics with Insane: A Versatile Tool for Generating Custom Membranes for Molecular Simulations. *J. Chem. Theory Comput.* **2015**, *11*, 2144−2155.
(54) Delemotte, L.; Dehez, F.; Treptow, W.; Tarek, M. Modeling Membranes under a Transmembrane Potential. *J. Phys. Chem. B* **2008**, *112*, 5547−5550.
(55) Lin, X.; Nair, V.; Zhou, Y.; Gorfe, A. A. Membrane Potential and Dynamics in a Ternary Lipid Mixture: Insights from Molecular Dynamics Simulations. *Phys. Chem. Chem. Phys.* **2018**, *20*, 15841−15851.
(56) Lin, X.; Zhang, S.; Ding, H.; Levental, I.; Gorfe, A. A. The Aliphatic Chain of Cholesterol Modulates Bilayer Interleaflet Coupling and Domain Registration. *FEBS Lett.* **2016**, *590*, 3368−3374.
(57) Lukat, G.; Krüger, J.; Sommer, Br., Apl@ Voro: A Voronoi-Based Membrane Analysis Tool for Gromacs Trajectories. *J. Chem. Inf. Model.* 2013, *53*, 2908−2925.
(58) Wei, C.; Pohorille, A. Flip-Flop of Oleic Acid in a Phospholipid Membrane: Rate and Mechanism. *J. Phys. Chem. B* **2014**, *118*, 12919−12926.
(59) Wang, Y. H.; Collins, A.; Guo, L.; Smith-Dupont, K. B.; Gai, F.; Svitkina, T.; Janmey, P. A. Divalent Cation-Induced Cluster Formation by Polyphosphoinositides in Model Membranes. *J. Am. Chem. Soc.* **2012**, *134*, 3387−3395.
(60) Yang, H.; Wang, L.; Yuan, B.; Yang, K.; Ma, Y. Adhesion of an Ultrasmall Nanoparticle on a Bilayer Membrane Is Still Size and Shape Dependent. *J. Mater. Sci. Technol.* **2015**, *31*, 660−663.
(61) Lin, X.; Li, Y.; Gu, N. Nanoparticle's Size Effect on Its Translocation across a Lipid Bilayer: A Molecular Dynamics Simulation. *J. Comput. Theor. Nanosci.* **2010**, *7*, 269−276.
(62) Ackerman, D. G.; Feigenson, G. W. Multiscale Modeling of Four-Component Lipid Mixtures: Domain Composition, Size, Alignment, and Properties of the Phase Interface. *J. Phys. Chem. B* **2015**, *119*, 4240−4250.
(63) Wassall, S. R.; Stillwell, W. Polyunsaturated Fatty Acid-Cholesterol Interactions: Domain Formation in Membranes. *Biochim. Biophys. Acta, Biomembr.* **2009**, *1788*, 24−32.
(64) Abankwa, D.; Gorfe, A. A.; Inder, K.; Hancock, J. F. Ras Membrane Orientation and Nanodomain Localization Generate Isoform Diversity. *Proc. Natl. Acad. Sci.* **2010**, *107*, 1130−1135.
(65) Aksimentiev, A.; Schulten, K. Imaging A-Hemolysin with Molecular Dynamics: Ionic Conductance, Osmotic Permeability, and the Electrostatic Potential Map. *Biophys. J.* **2005**, *88*, 3745−3761.
(66) Bruhn, D. S.; Lomholt, M. A.; Khandelia, H. Quantifying the Relationship between Curvature and Electric Potential in Lipid Bilayers. *J. Phys. Chem. B* **2016**, *120*, 4812−4817.
(67) Lin, J.; Alexander-Katz, A. Cell Membranes Open "Doors" for Cationic Nanoparticles/Biomolecules: Insights into Uptake Kinetics. *ACS Nano* **2013**, *7*, 10799−10808.
(68) Sotomayor, M.; Vásquez, V.; Perozo, E.; Schulten, K. Ion Conduction through Mscs as Determined by Electrophysiology and Simulation. *Biophys. J.* **2007**, *92*, 886−902.
(69) Li, H.; Chowdhary, J.; Huang, L.; He, X.; MacKerell, A. D.; Roux, B. Drude Polarizable Force Field for Molecular Dynamics Simulations of Saturated and Unsaturated Zwitterionic Lipids. *J. Chem. Theory Comput.* **2017**, *13*, 4535−4552.
(70) Basdevant, N.; Dessaux, D.; Ramirez, R. Ionic Transport through a Protein Nanopore: A Coarse-Grained Molecular Dynamics Study. *Sci. Rep.* **2019**, *9*, No. 15740.
(71) Sundelacruz, S.; Levin, M.; Kaplan, D. L. Role of Membrane Potential in the Regulation of Cell Proliferation and Differentiation. *Stem Cell Rev. Rep.* **2009**, *5*, 231−246.
(72) Levental, K. R.; Surma, M. A.; Skinkle, A. D.; Lorent, J. H.; Zhou, Y.; Klose, C.; Chang, J. T.; Hancock, J. F.; Levental, I. Ω-3 Polyunsaturated Fatty Acids Direct Differentiation of the Membrane Phenotype in Mesenchymal Stem Cells to Potentiate Osteogenesis. *Sci. Adv.* **2017**, *3*, No. eaao1193.

https://doi.org/10.1021/acs.jcim.2c00074
J. Chem. Inf. Model. XXXX, XXX, XXX−XXX

(73) Kinnun, J. J.; Bittman, R.; Shaikh, S. R.; Wassall, S. R. Dha Modifies the Size and Composition of Raftlike Domains: A Solid-State 2h Nmr Study. *Biophys. J.* **2018**, *114*, 380−391.
(74) Yee, S. M.; Lorenz, C. D. On the Structure and Flip-Flop of Free Docosahexaenoic Acid in a Model Human Brain Membrane. *J. Phys. Chem. B* **2021**, *125*, 8038−8047.
(75) Pedroni, V.; Sierra, M.; Alarcón, L.; Verde, A.; Appignanesi, G.; Morini, M. J. B. eB. A.-B. A Certain Proportion of Docosahexaenoic Acid Tends to Revert Structural and Dynamical Effects of Cholesterol on Lipid Membranes. *Biochim. Biophys. Acta, Biomembr.* **2021**, *1863*, No. 183584.
(76) Wassall, S. R.; Stillwell, W. Polyunsaturated Fatty Acid-Cholesterol Interactions: Domain Formation in Membranes. *Biochim. Biophys. Acta, Biomembr.* **2009**, *1788*, 24−32.
(77) Nickels, J. D.; Smith, J. C.; Cheng, X. Lateral Organization, Bilayer Asymmetry, and Inter-Leaflet Coupling of Biological Membranes. *Chem. Phys. Lipids* **2015**, *192*, 87−99.
(78) Tian, J.; Nickels, J.; Katsaras, J.; Cheng, X. Behavior of Bilayer Leaflets in Asymmetric Model Membranes: Atomistic Simulation Studies. *J. Phys. Chem. B* **2016**, *120*, 8438−8448.
(79) Bennett, W. F. D.; MacCallum, J. L.; Hinner, M. J.; Marrink, S. J.; Tieleman, D. P. Molecular View of Cholesterol Flip-Flop and Chemical Potential in Different Membrane Environments. *J. Am. Chem. Soc.* **2009**, *131*, 12714−12720.

https://doi.org/10.1021/acs.jcim.2c00074
J. Chem. Inf. Model. XXXX, XXX, XXX−XXX